*Journal of The Electrochemical Society*, **148** (10) G576-G580 (2001)
0013-4651/2001/148(10)/G576/5/$7.00 © The Electrochemical Society, Inc.

# A Photoelectrochemical Study of the GdMg Hydride Switchable Mirror

**M. Di Vece,[a,z] P. van der Sluis,[b] A.-M. Janner,[b] and J. J. Kelly[a,*]**

[a]*Debye Institute, Physics and Chemistry of Condensed Matter, Utrecht University, 3508 TA Utrecht, The Netherlands*
[b]*Philips Research, 5656 AA Eindhoven, The Netherlands*

A significant chemical stability has allowed us to perform photoelectrochemical measurements on the semiconducting state of the GdMg hydride system. With electrical impedance spectroscopy we confirm that GdMg hydride in the transparent state is an n-type semiconductor. The donor density was estimated to be $5 \times 10^{21}$ $cm^{-3}$. Impedance measurements give information about the potential distribution at the semiconductor/solution interface. Photocurrent was observed in the transparent state. It is proposed that photoanodic etching of the GdMg hydride at high light intensities occurs along grain boundaries, leading to inhomogeneous destruction of the film.
 [DOI: 10.1149/1.1401081] 

Manuscript submitted April 2, 2001; revised manuscript received May 16, 2001. Available electronically September 4, 2001.

Rare earth metal hydride films have unusual electrical and optical properties. On going from the dihydride to the trihydride state these systems show a reversible metal-to-insulator (semiconductor) transition. As expected, the metal is optically opaque while the insulator is transparent.[1] These properties open the way to novel applications such as switchable mirrors.

Stoichiometric trihydride cannot be formed when the hydrogen loading pressure is about 1 bar. The hydrogen vacancies at the octrahedral sites may act as donors, as proposed by Libowitz,[2] contributing electrons to the conduction band by thermal excitation. As a result, these materials should be n-type. For $YH_{3-\delta}$ at 1 bar of hydrogen pressure $\delta$ is about 0.1; from this the donor density $N_D$, which should be equal to the concentration of defects, can be estimated to be $2 \times 10^{21}$ $cm^{-3}$. Hall effect[3] and transmission spectra measurements[4] show the charge carrier density to be in the order of $10^{19}$ $cm^{-3}$. For $GdH_{3-\delta}$ a charge carrier density of $3.7 \times 10^{20}$ $cm^{-3}$ has been estimated by Lee and Lin.[5] The difference between the donor density and charge carrier density can be explained by the deep level of the donors, which results in only a fraction of the donors being ionized.

The lanthanide trihydrides are yellow in transmission and have low reflection in the metallic state. For technological applications, however, color neutrality and a high reflection ratio are desirable. Van der Sluis *et al.*[6] showed that this can be achieved by alloying with magnesium. A composition of 40% gadolinium and 60% magnesium is suitable and was used in our experiments.

Most thin film switchable mirror experiments are performed with a caplayer of palladium to prevent oxidation and enhance hydrogenation kinetics. Hydrogenation can be accomplished electrochemically[7] in a 1 M KOH solution, according to the reactions

$$H_2O + e^- \rightarrow H_{ad} + OH^-$$

$$MH_x + H_{ad} \rightarrow MH_{x+1}$$

The adsorbed hydrogen diffuses into the material; the concentration is proportional to the transferred charge. Since the trihydride is a semiconductor it should be possible, in principle, to apply (photo)-electrochemical techniques to study the system. Di Quarto *et al.*[8] have used photocurrent measurements to investigate the hydride produced on bulk yttrium during corrosion in acidic solution. They concluded that a semiconductor phase $YH_{3-\delta}$ is formed with a bandgap similar to that of the trihydride formed in the gas-phase loading of the metal. They used these measurements to speculate on the energetics of the $Y/YH_{3-\delta}$/aqueous system. Use of the bulk electrode under corrosion conditions, however, limits the stability of the system. In this work we describe an electrochemical study of thin GdMg alloy layers. The stability of this system enabled us to perform photocurrent and impedance measurements in conjunction with *in situ* optical measurements. The results give information about the semiconducting properties of the alloy. In addition, a characteristic photocorrosion process is described.

## Experimental

The geometry of the working electrode is shown in Fig. 1. An indium tin oxide (ITO) layer on glass was used as substrate. To ensure good adhesion of the GdMg alloy a 0.5 nm thick magnesium layer was evaporated onto the ITO. The active polycrystalline layer had a Gd/Mg ratio of 38/62 and a thickness of 218 nm, topcoated with a thin palladium layer (nominal thickness 10 nm). For convenience we omit the composition index, *i.e.*, we denote $Gd_{38}Mg_{62}$ simply by GdMg. The active film covered only part of the ITO surface to allow a back contact to the film via the ITO. The layers were deposited by evaporation at $10^{-7}$ mbar base pressure and analyzed with Rutherford backscattering (RBS) to determine thickness and composition. In the experiments described in this work the initial state of the electrode was $GdH_2Mg$, because the formation enthalpy of the irreversibly formed $GdH_2$ is much lower than that of $MgH_2$. $GdH_2Mg$ was formed by galvanostatically loading the GdMg sample in the electrochemical setup. From this state the sample could be reversibly loaded to $GdH_3MgH_2$.

The sample geometry allows impedance measurements for which the electrical contact should always be on the bulk material. The conductivity of the ITO is at least three times that of the film in the semiconducting state. A platinum lead was fixed with silver glue

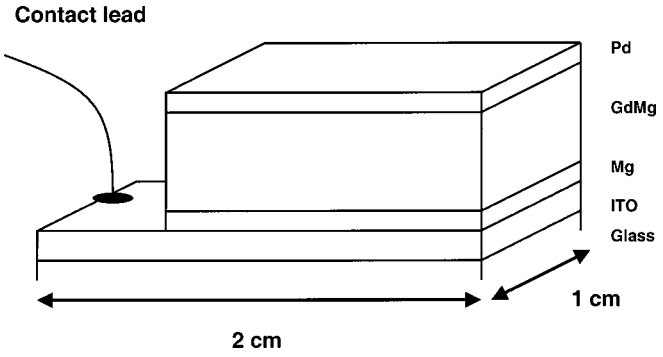


**Figure 1.** Geometry of the electrode. The connection to the potentiostat is made with a platinum lead on the ITO.

* Electrochemical Society Active Member.
z E-mail: m.divece@phys.uu.nl

(2400 circuit works conductive epoxy, Agar Scientific) on the free ITO surface, and both the lead and the ITO were protected from the solution by Apiezon. The active surface area was 1.3 $cm^2$. The electrical contact between the ITO substrate and the semiconductor layer was ohmic.

A two-compartment electrochemical glass cell was used for the measurements. The working electrode was positioned together with a saturated calomel reference electrode (SCE) in one compartment, and a platinum counter electrode was placed in the other compartment. All potentials are given with respect to SCE. To eliminate the possible influence of chloride ions during photocorrosion, we confirmed the results with a Hg/HgO reference electrode. Argon gas was bubbled through both chambers. The glass cell had windows on both sides through which we could illuminate the sample and also measure transmission. For illumination, a 500 W HgXe lamp (Oriel) was used. Transmission was measured with a diode laser (Vector, 670 nm) and a standard photodiode. All electrochemical experiments were performed in a 1 M KOH electrolyte solution at room temperature.

A potentiostat/galvanostat (EG&G Princeton Applied Research (PAR) 273A) was used in combination with a frequency response analyzer (Schlumberger-Solartron SI 1255). Photocurrent was measured with a Stanford Research Systems SR830 DSP lock-in amplifier and a SR540 chopper operated at 379 Hz. This setup was computer-controlled by in-house developed programs (LabView). Impedance data were fitted with the "Equivalent Circuit Program"[9,10] provided by B. A. Boukamp, University of Twente, The Netherlands.

The surface of the samples was examined with an XL30EFG scanning electron microscope (SEM, Philips). Energy-dispersive analysis by X-ray (EDAX) was used for element analysis during SEM operation. Besides SEM and EDAX, X-ray photoelectron spectroscopy (XPS) was also used to inspect the surface of etched samples. The XPS data were obtained with a Vacuum Generators XPS system, using a CLAM-2 hemispherical analyzer for electron detection.

## Results

*Voltammetry*.—Curve A of Fig. 2 shows a cyclic voltammogram of the $GdH_2Mg$ sample in a 1 M KOH solution. The scan toward negative potentials was started at 0 V. At −0.9 V, loading of the sample begins as the current becomes strongly cathodic. After a slight decrease at around −1.3 V, the cathodic current increases again due to hydrogen evolution. The scan is reversed at −1.55 V. The transmission of the electrode (curve B, Fig. 2) is low in the potential range between 0 and −1.4 V. After −1.4 V the transmission starts to increase and continues to increase when the scan is reversed at −1.55 V. It is clear that in the return scan there is a potential range of 0.6 V in which the transparent state persists, since

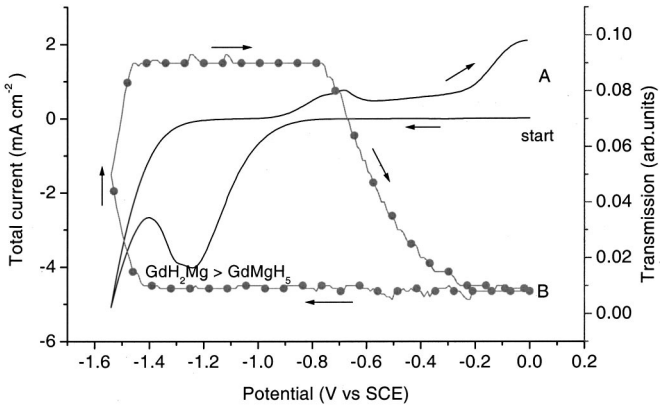


**Figure 2.** The potential dependence of the current density (A) and transmission (B) of a GdMg electrode in a 1 M KOH solution. Scan rate 8 mV $s^{-1}$.

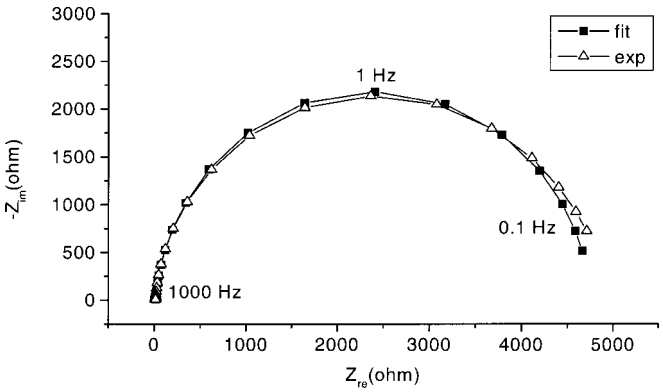


**Figure 3.** Electrical impedance plot at −1.1 V in the transparent state: (△) experimental values, (■) values from a fit with an equivalent circuit consisting of a resistor R1 in series with a resistor R2 and CPE *Q*, parallel to each other. R1 = 12 Ω, R2 = 4.8 kΩ (1.6%), Q = $3.7 \times 10^{-5}$ F (1.6%), $n$ = 0.95 (0.3%).

the transmission decreases only at −0.8 V, gradually returning to its original value. At −0.9 V a small anodic current peak is observed. The anodic current increases significantly only at −0.3 V. At the potential limit of the scan (0 V), the film has not yet released all the hydrogen that can be reversibly transported to and from the film, since a considerable current is still flowing. At lower scan rates this effect vanishes. However, photocurrent measurements force us to use this scan rate to avoid premature dissolution of the film, as we discuss later. Because the film remains in the transparent state over a considerable potential range, it is possible to perform various experiments on the semiconductor as a function of potential.

*Impedance*.—In Fig. 3, electrical impedance measurements are shown for the electrode in the fully loaded state at −1.1 V (*vs.* SCE). The imaginary component of the impedance is plotted as a function of the real component. For the frequency range of these measurements, the semicircle can be represented by an equivalent electrical circuit of a resistor in series with a parallel circuit of a constant phase element (CPE) and a resistor. The expression for the CPE is

$$Z_{\mathrm{CPE}} = (j\omega)^{-n}/Y_0$$

where ω is the frequency and $Y_0$ is a parameter containing elements which depend on the electrochemical system. The value of $n$ (0.95) is very close to 1, indicating that the CPE is almost equivalent to a capacitor. A fit with the Boukamp program gives an accuracy better than 2%. The slight deviation of $n$ from 1 is responsible for frequency dispersion. This kind of dispersion is not uncommon and can be caused by a variety of phenomena, like surface roughness, surface states,[11] and/or deep-lying impurity levels.[12] From the absence of a Warburg component at low frequencies we conclude that there is no limitation due to mass transport within the film. Therefore, the hydrogen concentration in the film during the measurement remains constant. The high-frequency limit of the impedance is determined by the ohmic resistance (order of 10 Ω) of the film, liquid electrolyte, and the external circuit. The parallel resistance allows for a small "leakage current" through the interface.[14]

In Fig. 4, $C^{-2}$ is plotted as a function of potential. The capacitance was calculated from the measured impedance, with an equivalent circuit consisting of a capacitor parallel to a resistor. This procedure was performed for three frequencies. There are three regimes in this plot. At the most negative potentials (A) the capacitance at a given frequency is essentially independent of the potential. This regime is followed by two "linear" ranges with different slope (B and C).

*Photocurrent*.—To measure photocurrent the sample was illuminated with a HgXe lamp (with water filter and 25% neutral density

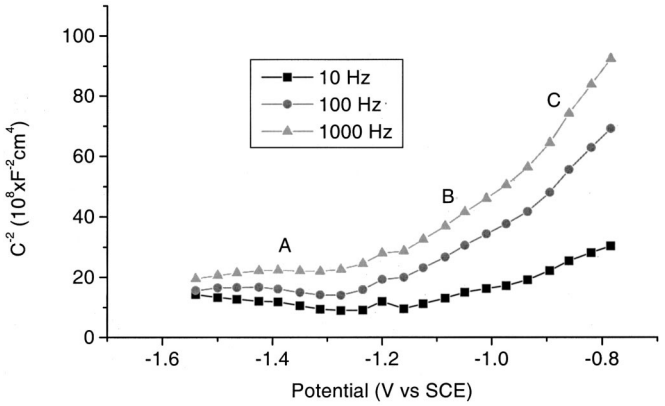


**Figure 4.** The potential dependence of $C^{-2}$ at three measuring frequencies.

filter). Figure 5 shows the photocurrent (B) measured simultaneously with the total current (A) as a function of the potential. Again, the scan starts at 0 V, with the electrode in the metallic state ($GdH_2Mg$). Up to −0.9 V a small offset in the measured photocurrent is observed. From −0.9 V, in the opaque state, the photocurrent increases up to the potential at which the scan is reversed. While the film becomes transparent (compare with Fig. 2) a strong photocurrent is measured until the film again becomes opaque. Note the small decrease of photocurrent just before the potential limit of the scan is reached and after the scan is reversed. We find a photocurrent onset (in the wavelength domain) at 440 nm. This is in accordance with transmission spectra reported by van der Sluis.[6]

*Photocorrosion*.—Under illumination with the full intensity of the lamp a characteristic degradation of the electrode is observed. Figure 6A shows a SEM photograph of a surface which was illuminated for 20 min at −1.1 V (SCE). Holes, many of them circular in shape, have been opened in the layer. These holes seem to be caused by peeling or detachment of portions of the layer. In certain cases, the detached region can still be seen close to its parent hole. Transients of the photocurrent and total current measured during degradation under full illumination are shown in Fig. 7. Before illumination, the film was completely loaded and transparent. The photocurrent (top) appears immediately on illumination, goes through a maximum at about 200 s, and decreases after 1000 s to a lower value. Integration of the photocurrent gives a charge of about 0.13 mC/cm$^2$. The total current is clearly anodic (bottom) and starts at about 30 s after the start of the photocurrent. The charge under the peak is 4.2 mC/cm$^2$.

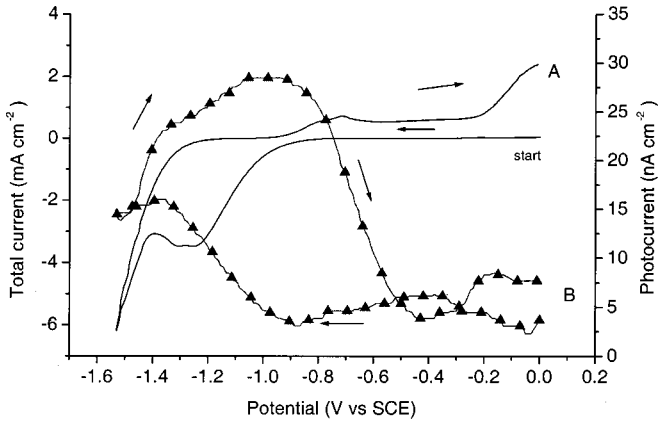


**Figure 5.** The potential dependence of (A) current density and (B) photocurrent density of a GdMg electrode in a 1 M KOH solution. Scan rate 8 mV s$^{-1}$.

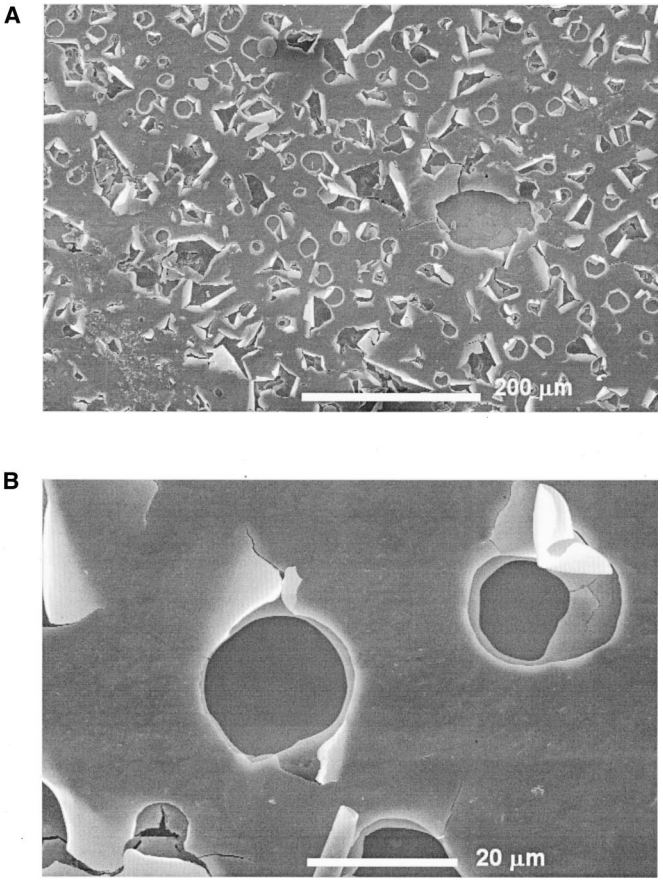


**Figure 6.** SEM of the GdMg film etched in a 1 M KOH solution under illumination at a potential of −1.1 V for 20 min.

In Fig. 6B a close-up of some circular holes can be seen. We inspected one such hole with EDAX. In the center we found no Gd, Mg, or Pd. Indium from the ITO substrate was detected. In the second layer we found Mg but no Gd or Pd; this is very likely from the adhesion layer and from magnesium due to separation out of the GdMg alloy. The outer surface contained all the elements (Gd, Mg, Pd) used.

An equivalent sample was etched in the same way as described previously for a longer time. During the rinsing process the film was completely detached from the substrate. XPS measurements on this ''bare'' surface showed neither palladium nor gadolinium were present. Magnesium was found, but evidently in an amount still undetectable by EDAX. We believe the presence of magnesium after etching results from the reaction of parts of the magnesium adhesion layer with the ITO. This magnesium therefore cannot be removed only by etching.

## Discussion

From the results presented in the previous section it is clear that the reversible transition of the GdMg hydride system from the metallic to the semiconductor state is accompanied by interesting changes in the electrical impedance. In addition, photocurrent is observed, as well as a photocorrosion effect with remarkable features. In this section we consider these results.

In Fig. 2 it is shown that the transmission begins to increase at −1.4 V. The charge passed at this point (0.24 C) is close to that necessary to convert the layer to the $GdH_3MgH_2$ state. Clearly, almost the complete layer must be converted for the film to become transparent.

In the voltammogram a current peak is observed in the reverse scan at −0.8 V. Although anodic current begins to flow at −1.0 V,

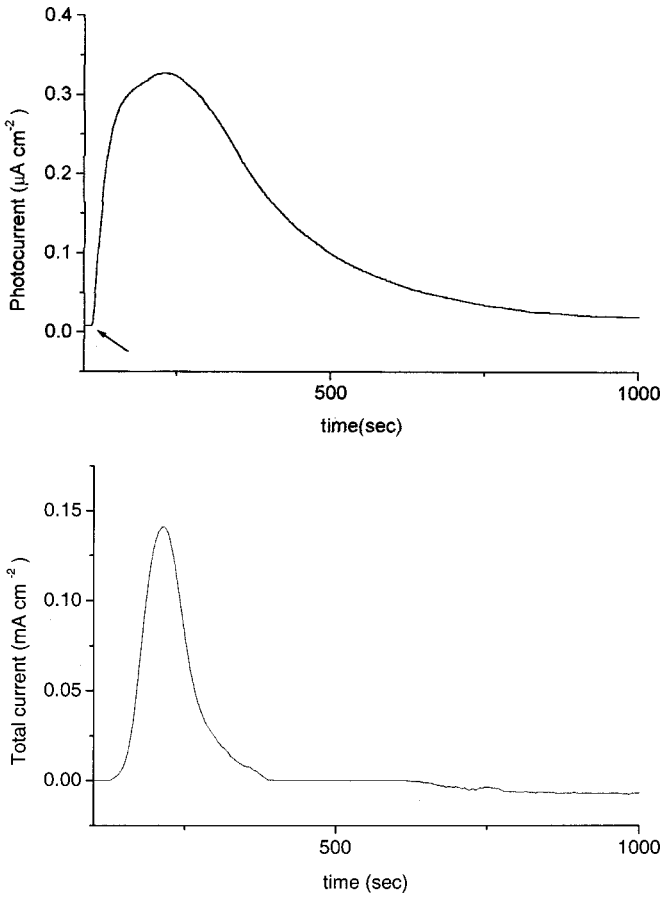


**Figure 7.** Current transient corresponding to the experiment of Fig. 6: (top) photocurrent and (bottom) total current. Photocurrent onset occurs instantaneously (see arrow) while the total current shows a delayed response (30 s).

the transmission remains constant. Very likely the current in this range corresponds to oxidation of hydrogen adsorbed at the palladium surface or removal of absorbed hydrogen from the palladium islands. The decrease in transmission shows that the film starts to unload at −0.75 V. That this process is rather slow is clear from the low anodic current up to −0.3 V. At this potential the rate of unloading increases significantly.

The results shown in Fig. 3 for a more negative potential (−1.1 V) indicate a simple equivalent circuit consisting of a resistor in series with a capacitance parallel to a resistor. The capacitance depends strongly on the applied potential above −1.2 V (Fig. 4), as would be expected for a semiconductor electrode under depletion conditions. In this case the impedance is described by Mott-Schottky theory, which predicts a linear relationship between $C^{-2}$ and the potential

$$C_{sc}^{-2} = (2/eN_D\varepsilon_r\varepsilon_0)\left(U - U_{FB} - \frac{kT}{q}\right)$$

$N_D$ is the donor density, $C_{sc}$ is the space charge capacitance, $q$ the electronic charge, and $\varepsilon_r$ denotes the dielectric constant for which we take the value of fully hydrided $Gd_{42}Mg_{58}$.[13]

A plot of our results in Fig. 4 indeed gives linear ranges for potentials above −1.2 V. The positive slopes (B and C) show that the electrode must be an n-type semiconductor. The results given in Fig. 4 are, however, more complicated than what is normally found with semiconductor electrodes. Under depletion conditions (V > −1.4 V) three linear ranges are observed. At lower potential $C^{-2}$ becomes almost independent of potential (A). According to the Mott-Schottky relationship the donor density can be calculated from the slope of the $C^{-2}$ *vs. U* plot. The value obtained from the results in Fig. 4 at positive potentials and 1000 Hz is $5 \times 10^{21}$ cm$^{-3}$. Compared to reported free carrier densities for conventional semiconductors, this donor density seems unexpectedly high. It probably indicates ionization of all donors in the system during the experiment in depletion. One has to take into account the fact that the energy difference between the conduction band and the donor level may be large, *e.g.*, in the case of $YH_{3-\delta}$, the donor level is 0.13 eV[4] below the conduction bandedge. This results in the ionization of just a fraction of the donors at room temperature and stable conditions. Assuming a similar donor level in this case, we find a charge carrier density of about $10^{19}$ to $10^{20}$ cm$^{-3}$. This resembles the value reported for yttrium trihydride[1] and is similar to the charge carrier density reported for $GdH_{3-\delta}$.[5]

In the potential range (A) between −1.55 and −1.2 V the capacitance is dependent on the frequency but is essentially independent of the potential. This indicates a pinning of the Fermi level due to surface states.[14] In that case the applied potential changes only the Helmholtz capacitance. The band bending within the space-charge layer of the semiconductor remains unchanged in this range. As a result, extrapolation of the linear Mott-Schottky plots to the potential at which $C^{-2} = 0$ (−1.4 V) does not yield the true flatband potential value. The true flatband condition is obtained at a potential more negative than −1.55 V; this is beyond the reach of the present measurements because of strong hydrogen evolution.

The interpretation of our impedance results is based on the case of a semiconductor/electrolyte interface. The present system is obviously more complicated. There is palladium on the surface, probably as islands. The surface is partially covered by an oxide/hydroxide layer which may also extend under the islands.[15,16] The results, however, clearly show the importance of the presence of a depletion layer within the semiconductor. As would be expected, a photocurrent is observed for the semiconductor under strong depletion conditions (Fig. 5). Electrons and holes, generated by light, are separated by the electric field of the depletion layer. The holes are used for an oxidation reaction at the semiconductor/electrolyte interface. The electrons are detected as photocurrent in the external circuit. In contrast to the transmission, for which an increase is observed only when the layer has been almost completely loaded (Fig. 2), photocurrent is observed at considerably more positive potential (−0.9 V). We assume that because of slow diffusion of hydrogen, a concentration gradient is established at the semiconductor/solution interface within the film. As a result, a thin semiconducting layer is formed which gradually grows in thickness. A photocurrent is expected as soon as the semiconducting layer has a thickness comparable to that of the depletion layer. The decrease of the photocurrent just before the scan is reversed and the delayed onset on scan reversal indicates the disappearance of the depletion layer ($V < V_{FB}$). From the photocurrent and impedance measurements we deduce that the true flatband potential is more negative than −1.6 V. This would place the conduction bandedge before Fermi level pinning, at an energy of less than 3.3 eV with respect to the vacuum level.[14] The photocurrent disappears as the film returns to the metallic state.

The corrosion observed under illumination (Fig. 6) suggests that the photocurrent is due to the photoanodic oxidation of the layer similar to the results reported for yttrium in Ref. 17. A possible mechanism for this reaction is

$$GdH_3 + 6h^+ + 6\ OH^- = Gd(OH)_3 + 3H_2O$$

$$MgH_2 + 4h^+ + 4\ OH^- = Mg(OH)_2 + 2H_2O$$

The gadolinium and magnesium hydroxide formed in this way are dissolved in the electrolyte.[18] In order to explain the highly unusual form of corrosion, we suggest that at high light intensity photoanodic attack occurs preferentially at defects and/or grain boundaries. When GdMg is removed along the boundary, the magnesium adhesion layer is exposed to the solution. The metal is oxidized anodi-

cally, giving rise to the anodic dark current transient shown in Fig. 7. With the removal of the magnesium, the GdMg hydride film becomes detached. Because of the stress in the film due to hydrogen loading, the layer may ''break away'' completely, as is clear in Fig. 6B. When the solution reaches the magnesium layer at a single point a concentric hole is expected. This mechanism explains the time lag between onset of the total current and the photocurrent. In addition, the charge involved in the total current transient is of the same order of magnitude as that necessary to oxidize the magnesium adhesion layer.

## Conclusions

The cyclic voltammogram shows that the transparent state of $Gd_{38}Mg_{62}$, once created at low potentials, remains relatively stable up to much higher potentials. This enables the investigation of the properties of the semiconducting state as a function of potential. Impedance measurements confirm the stability of the semiconductor since no mass transport can be detected in the transparent state. Application of the Mott-Schottky relation provides us with a donor density comparable to values estimated for gadolinium and known charge carrier densities for comparable materials. The n-type nature of this semiconductor is also confirmed by the positive slope of the Mott-Schottky plot. The flatband potential indicated by the Mott-Schottky relation is consistent with the photocurrent experiments. Photoanodic etching is possible. However, etching is not homogeneous at high light intensities and anodic oxidation of the magnesium adhesion layer initiates delamination of the film.

## Acknowledgments

The authors thank E. M. H. Evens and J. M. Kerkhof for preparation of the samples, X. Xia for SEM investigation, O. L. J. Gijzeman for XPS inspection, and E. S. Kooij from the Vrije Universiteit, Amsterdam, for stimulating discussion. The work described here was supported by the Council for Chemical Sciences (CW), with financial aid from the Netherlands Organization for Scientific Research (NWO) and the Netherlands Foundation for Technical Research (STW).

*The Debye Institute, Utrecht University, assisted in meeting the publication costs of this article.*

## References

1. J. N. Huiberts, R. Griessen, J. H. Rector, R. J. Wijngaarden, J. P. Dekker, D. G. de Groot, and N. J. Koeman, *Nature*, **380**, 231 (1996).
2. G. G. Libowitz, *Ber. Bunsen-Ges. Phys. Chem.*, **76**, 837 (1972).
3. J. N. Huiberts, Ph.D. Thesis, Vrije Universiteit Amsterdam (1995).
4. M. W. Lee and W. P. Shin, *J. Appl. Phys.*, **86**, 6798 (1999).
5. M. W. Lee and C. H. Lin, *J. Appl. Phys.*, **87**, 7798 (2000).
6. P. van der Sluis, M. Ouwerkerk, and P. A. Duine, *Appl. Phys. Lett.*, **70**, 3356 (1997).
7. P. H. L. Notten, M. Kremers, and R. Griessen, *J. Electrochem. Soc.*, **143**, 3348 (1996).
8. F. Di Quarto, M. C. Romano, S. Piazza, and C. Sunseri, *Electrochim. Acta*, **44**, 4051 (1999).
9. B. A. Boukamp, *Solid State Ionics*, **18&19**, 136 (1986).
10. B. A. Boukamp, *Solid State Ionics*, **20**, 31 (1986).
11. G. Nogami, *J. Electrochem. Soc.*, **133**, 525 (1986).
12. G. Nogami, *J. Electrochem. Soc.*, **129**, 2219 (1982).
13. K. von Rottkay, M. Rubin, F. Michalak, R. Armitage, T. Richardson, J. Slack, and P. A. Duine, *Electrochim. Acta*, **44**, 3093 (1999).
14. S. R. Morrison, *Electrochemistry at Semiconductor and Oxidized Metal Electrodes*, Plenum Press, New York (1980).
15. S. J. van der Molen, J. W. J. Kerssemakers, J. H. Rector, N. J. Koeman, B. Dam, and R. Griessen, *J. Appl. Phys.*, **86**, 6107 (1999).
16. A.-M. Janner and P. van der Sluis, in *Solid-State Ionic Devices*, E. D. Wachsman, J. R. Akridge, M. Liu, and N. Yamazoe, Editors, PV 99-13, p. 289, The Electrochemical Society Proceedings Series, Pennington, NJ (1999).
17. P. H. L. Notten, *Recent Res. Dev. Electrochem.*, **3**, 1 (2000).
18. M. Pourbaix, *Atlas of Electrochemical Equilibria in Aqueous Solutions*, Pergamon Press, Elmsford, NY (1966).